Supplement material for

Paleoseismic trenching on slip-partitioned surface ruptures associated with the 2016 Kumamoto earthquake

Daisuke Ishimura [1,*], Naoya Takahashi [2], Hiroyuki Tsutsumi[3], Shin'ichi Homma[4], Sakae Mukoyama[4], and Toshihiko Ichihara[5]

[1] Department of Earth Sciences, Chiba University, 1-33 Yayoi-cho, Inage-ku, Chiba 263-8522, Japan
[2] Department of Earth Science, Tohoku University, 6-3 Aoba, Aoba-ku, Sendai 980-8578, Japan
[3] Department of Environmental Systems Science, Doshisha University, 1-3 Tataramiyakodani, Kyotanabe, Kyoto 610-0394, Japan
[4] Department of Research & Development of Kokusai Kogyo Co., Ltd., 2-24-1 Harumi-cho, Fuchu, Tokyo 183-0057, Japan
[5] Faculty of Social and Cultural Studies, Kyusyu University, 744 Motooka, Nishi-ku, Fukuoka 819-0395, Japan
[*]Corresponding author: ishimura@chiba-u.jp

The PDF file includes:

Figs S1 to S2
Tables S1 to S5
Materials 1 to 2

Supplement Figure S1

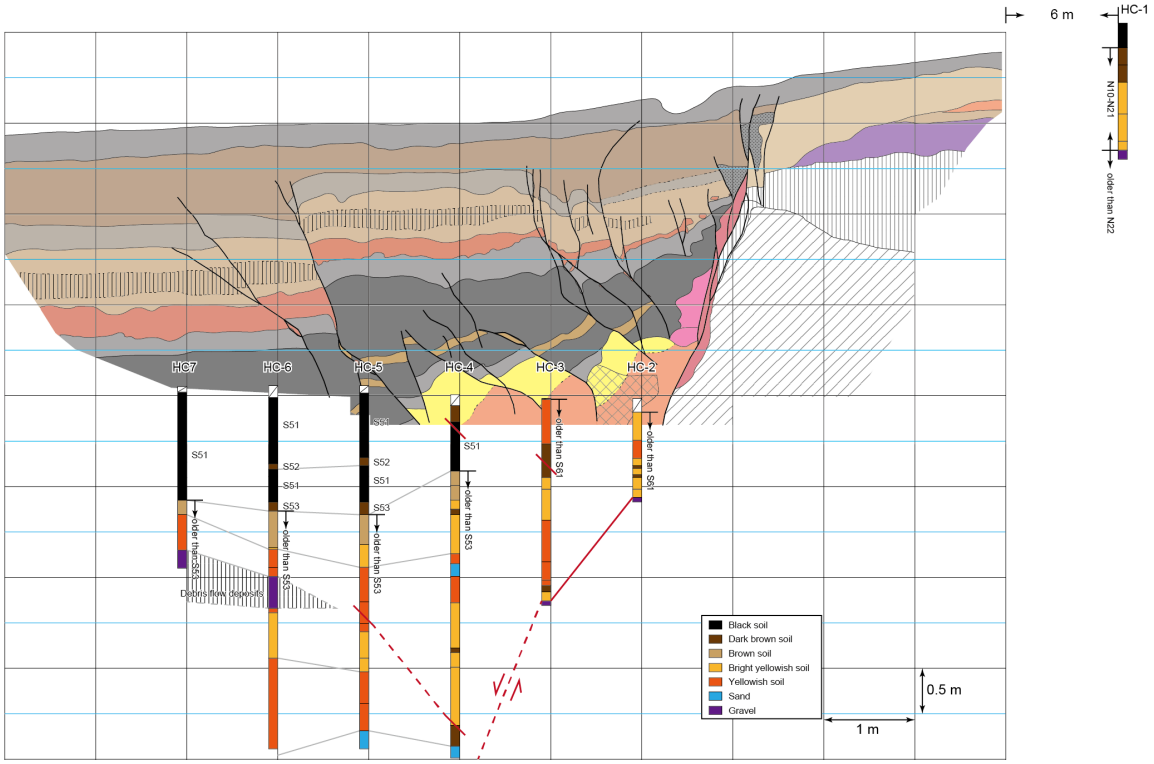

Figure S1. Subsurface structure from the trench floor based on hand coring survey. Coring sites are shown in Fig. 3b.

Supplement Figure S2

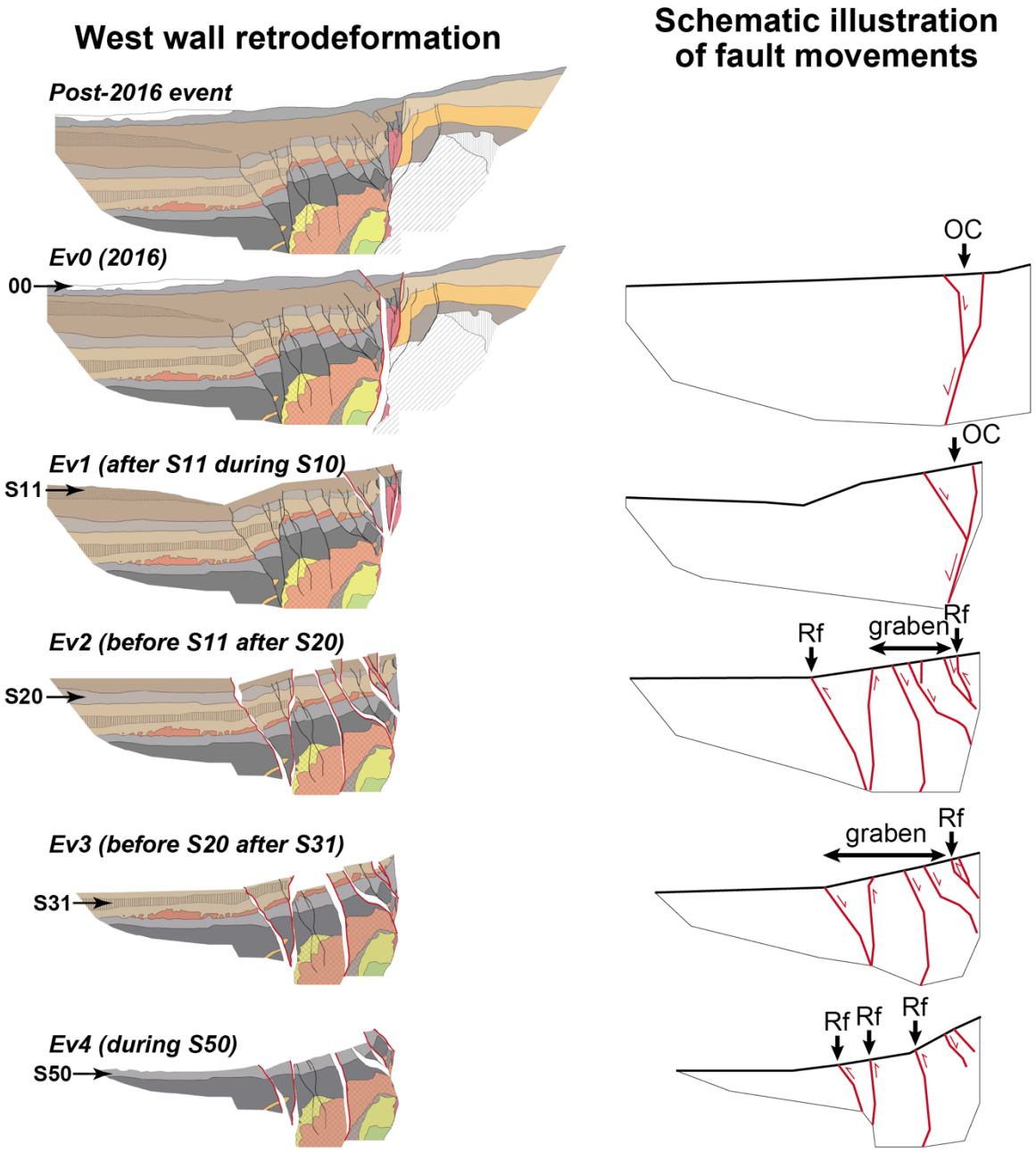

Figure S2. Retrodeformation of the faults and schematic illustration of fault movements on the east wall. The left figures show reconstructions of the displacement for each event, and the right figures show the faults that were active during that event. Rf: reverse fault, OC: open crack.

Table S1 Characteristics of the major tephras since ca. 30 ka in the study area

Tephra name	Source	Age [ka]	VEI	Morphology of shards	Refractive index (mode)	Reference
Nakadake N2 (N2S)	Aso	1.5	3	-	>1.550	2, 3
Ojodake scoria (OjS)	Aso	3.6	3	-	-	2
Kishimadake scoria (KsS)	Aso	4	3	-	-	2
Aso central cone pumice 1 (ACP1)	Aso	4.1	-	-	-	2
Kikai-Akahoya (K-Ah)	Kikai caldera (southern Kyushu)	7.3	7	bw, pm	1.505-1.513 (1.510-1.512)	1
Aira-Tn (AT)	Aira caldera (southern Kyusyu)	30	7	bw	1.498-1.500	1, 4
Kusasenrigahama pumice (Kpfa)	Aso	30	5	-	-	2

bw: bubble wall type, pm: pumiceous type. VEI: Volcanic Explosivity Index (Newhall and Self, 1982). 1: Machida and Arai (2003), 2: Miyabuchi (2009), 3:

Table S2 Characteristics of the tephras sampled in the trench

Sample No.	Sample Location	Unit No. in trench	Grain composition Volcanic glass (%)	Morphology of shards	Refractive index (mode): measured number	Interpretation
1	West wall	S40	-	bubble wall type	1.510–1.512 (1.511): 31	K-Ah
2	North wall	N30	0.5	-	-	
3	North wall	N30	0.0	-	-	
4	North wall	N23	0.0	-	-	
5	North wall	N21	0.0	-	-	
6	North wall	N21	0.0	-	-	
7	North wall	N21	0.9	-	-	
8	North wall	N20	2.1	bubble wall type	1.496–1.500 (1.498): 29, 1.503: 1	AT rework
9	North wall	N11	1.6	bubble wall type	1.495–1.499 (1.498): 27, 1.503: 1, 1.510: 1, 1.513: 1	AT rework
10	North wall	N10	3.3	bubble wall type	1.497–1.500 (1.497–1.498): 17, 1.508–1.511 (1.510): 13	AT+K−Ah rework
11	North wall	N10	5.2	bubble wall type	1.497–1.499 (1.498): 7, 1.509–1.511 (1.510): 23	AT+K−Ah rework
12	North wall	N10	9.3	bubble wall type	1.497–1.499 (1.499): 9, 1.508–1.512 (1.510): 21	AT+K−Ah rework

Table S3 Major element compositions of volcanic glass shard samples and the AT tephra working standard

Sample name	SiO_2	TiO_2	Al_2O_3	FeO*	MnO	MgO	CaO	K_2O	Na_2O	*n*	Total**	Correlation
Sample No. 1	74.0	0.6	13.1	2.8	0.2	0.6	2.1	2.7	3.9	*17*	97.5	K–Ah
This study	0.7	0.1	0.2	0.2	0.1	0.1	0.2	0.1	0.1		0.9	
T1 (K-Ah)	74.0	0.6	13.0	2.8	0.2	0.6	2.1	2.8	4.0	*16*	96.5	–
Ishimura et al. (2022)	0.5	0.1	0.2	0.2	0.1	0.1	0.2	0.1	0.1		1.7	
AT	77.9	0.1	12.4	1.4	0.1	0.2	1.0	3.2	3.6	*12*	94.5	–
Working standard	0.3	0.1	0.1	0.1	0.1	0.0	0.1	0.1	0.1		1.1	

The number on the upper line is the mean value and that on the lower line is the standard deviation. Measured values were recalculated to 100% on a water–free basis. FeO*, total iron oxide as FeO. Total**, raw data before recalculation.

Table S4 SEM-EDS analysis results

		Normalized to 100%										
Sample	**Date analyzed**	**SiO2**	**TiO2**	**Al2O3**	**FeO**	**MnO**	**MgO**	**CaO**	**K2O**	**Na2O**	**Total**	**Analytical Total**
Sample No.1	2023/9/21	73.5	0.6	13.3	3.0	0.2	0.7	2.3	2.5	3.9	100.0	97.3
Sample No.1	2023/9/21	74.5	0.6	13.0	2.7	0.2	0.6	1.9	2.7	3.9	100.0	98.2
Sample No.1	2023/9/21	74.3	0.6	13.1	2.7	0.2	0.6	1.9	2.8	3.9	100.0	97.9
Sample No.1	2023/9/21	74.5	0.5	13.2	2.7	0.1	0.6	1.8	2.8	4.0	100.0	96.9
Sample No.1	2023/9/21	74.7	0.6	13.0	2.7	0.1	0.5	1.8	2.7	4.0	100.0	96.5
Sample No.1	2023/9/21	72.9	0.8	13.4	2.9	0.2	0.7	2.4	2.8	4.0	100.0	98.4
Sample No.1	2023/9/21	74.1	0.7	13.0	2.8	0.4	0.5	2.0	2.7	3.9	100.0	96.5
Sample No.1	2023/9/21	74.3	0.6	13.0	2.8	0.1	0.5	2.0	2.8	3.8	100.0	97.8
Sample No.1	2023/9/21	72.9	0.8	13.4	3.3	0.4	0.7	2.3	2.6	3.7	100.0	98.9
Sample No.1	2023/9/21	74.3	0.6	12.9	2.8	0.3	0.5	2.0	2.8	3.7	100.0	98.2
Sample No.1	2023/9/21	73.0	0.8	13.4	2.9	0.2	0.7	2.3	2.7	4.0	100.0	97.8
Sample No.1	2023/9/21	74.8	0.5	13.1	2.4	0.1	0.6	1.9	2.8	3.9	100.0	95.7
Sample No.1	2023/9/21	74.3	0.6	13.0	2.8	0.2	0.5	1.9	2.8	4.0	100.0	98.1
Sample No.1	2023/9/21	74.3	0.6	12.9	2.6	0.2	0.5	2.0	2.8	4.0	100.0	96.6
Sample No.1	2023/9/21	72.8	0.7	13.5	3.1	0.3	0.7	2.6	2.6	3.9	100.0	98.9
Sample No.1	2023/9/21	74.4	0.6	13.0	2.6	0.2	0.5	2.0	2.9	3.9	100.0	97.3
Sample No.1	2023/9/21	74.5	0.6	12.9	2.6	0.2	0.5	2.0	2.7	3.9	100.0	96.8
	Average	**74.0**	**0.6**	**13.1**	**2.8**	**0.2**	**0.6**	**2.1**	**2.7**	**3.9**		**97.5**
	SD	**0.7**	**0.1**	**0.2**	**0.2**	**0.1**	**0.1**	**0.2**	**0.1**	**0.1**		**0.9**
T1 in Ishimura et al. (2022)	2023/9/21	74.5	0.5	13.0	2.6	0.2	0.5	2.0	2.8	3.8	100.0	98.0
T1 in Ishimura et al. (2022)	2023/9/21	74.2	0.7	12.9	2.8	0.2	0.5	2.0	2.8	4.0	100.0	95.8
T1 in Ishimura et al. (2022)	2023/9/21	73.0	0.7	13.3	3.0	0.2	0.7	2.4	2.7	4.0	100.0	98.4
T1 in Ishimura et al. (2022)	2023/9/21	73.2	0.7	13.4	3.0	0.1	0.7	2.3	2.6	4.0	100.0	95.0
T1 in Ishimura et al. (2022)	2023/9/21	74.3	0.6	13.1	2.9	0.1	0.5	1.9	2.7	3.9	100.0	93.3
T1 in Ishimura et al. (2022)	2023/9/21	74.0	0.6	13.0	2.6	0.3	0.6	2.1	2.8	4.1	100.0	96.7
T1 in Ishimura et al. (2022)	2023/9/21	73.0	0.7	13.4	3.1	0.2	0.6	2.4	2.6	4.0	100.0	98.1
T1 in Ishimura et al. (2022)	2023/9/21	74.1	0.6	12.9	2.7	0.3	0.5	2.0	2.9	4.0	100.0	95.5
T1 in Ishimura et al. (2022)	2023/9/21	74.2	0.6	13.0	2.6	0.3	0.6	2.0	2.8	3.9	100.0	98.0
T1 in Ishimura et al. (2022)	2023/9/21	74.2	0.6	13.0	2.6	0.2	0.6	2.0	2.8	4.1	100.0	97.6
T1 in Ishimura et al. (2022)	2023/9/21	74.0	0.6	13.0	2.8	0.3	0.5	2.0	2.8	4.0	100.0	98.0
T1 in Ishimura et al. (2022)	2023/9/21	74.3	0.6	12.8	2.7	0.1	0.5	2.0	2.9	4.0	100.0	95.2
T1 in Ishimura et al. (2022)	2023/9/21	74.4	0.5	12.8	2.8	0.1	0.6	2.1	2.8	4.0	100.0	92.9
T1 in Ishimura et al. (2022)	2023/9/21	74.1	0.7	13.0	2.8	0.2	0.6	2.0	2.8	3.9	100.0	96.8
T1 in Ishimura et al. (2022)	2023/9/21	74.7	0.5	13.2	2.5	0.0	0.6	1.9	2.9	3.9	100.0	97.5
T1 in Ishimura et al. (2022)	2023/9/21	74.5	0.7	13.0	2.6	0.2	0.6	2.0	2.8	3.8	100.0	97.8
	Average	**74.0**	**0.6**	**13.0**	**2.8**	**0.2**	**0.6**	**2.1**	**2.8**	**4.0**		**96.5**
	SD	**0.5**	**0.1**	**0.2**	**0.2**	**0.1**	**0.1**	**0.2**	**0.1**	**0.1**		**1.7**

Table S4 SEM-EDS analysis results

Normalized to 100%

Sample	Date analyzed	SiO2	TiO2	Al2O3	FeO	MnO	MgO	CaO	K2O	Na2O	Total	Analytical Total
AT	2023/9/21	77.7	0.2	12.3	1.5	0.1	0.2	1.1	3.1	3.6	100.0	95.0
AT	2023/9/21	77.9	0.1	12.4	1.4	0.1	0.3	1.0	3.2	3.7	100.0	96.5
AT	2023/9/21	78.2	0.1	12.3	1.3	0.0	0.2	1.0	3.3	3.6	100.0	94.2
AT	2023/9/21	77.3	0.2	12.6	1.5	0.1	0.3	1.1	3.2	3.6	100.0	94.1
AT	2023/9/21	78.2	0.1	12.4	1.4	0.2	0.2	1.0	3.1	3.4	100.0	93.0
AT	2023/9/21	78.3	0.0	12.5	1.4	0.1	0.2	1.0	3.1	3.5	100.0	92.7
AT	2023/9/21	78.0	0.1	12.3	1.4	0.1	0.2	1.1	3.2	3.6	100.0	96.3
AT	2023/9/21	77.7	0.2	12.4	1.5	0.1	0.2	1.0	3.2	3.7	100.0	95.4
AT	2023/9/21	77.6	0.2	12.4	1.5	0.1	0.3	1.1	3.3	3.6	100.0	94.6
AT	2023/9/21	77.8	0.2	12.2	1.4	0.1	0.2	1.1	3.3	3.7	100.0	94.9
AT	2023/9/21	77.9	0.1	12.3	1.4	0.2	0.2	1.1	3.3	3.5	100.0	94.2
AT	2023/9/21	78.6	0.0	12.5	1.3	0.0	0.2	1.0	3.0	3.5	100.0	93.5
	Average	**77.9**	**0.1**	**12.4**	**1.4**	**0.1**	**0.2**	**1.0**	**3.2**	**3.6**		**94.5**
	SD	**0.3**	**0.1**	**0.1**	**0.1**	**0.1**	**0.0**	**0.1**	**0.1**	**0.1**		**1.1**

Table S5 Radiocarbon dates of samples from the trench

Sample No.	Lab. No.	Sample position (Unit No.)	Material	$\delta^{13}C$ [‰]	Conventional ^{14}C age [yr BP]	Calibrated age (2σ) [cal yr BP]
1	IAAA-181201	S50	sediment	-21.94 ± 0.23	8,634 ± 33	9679–9536 (95.4%)
2	IAAA-181202	S51 (upper)	sediment	-22.07 ± 0.29	11,722 ± 40	13743–13704 (6.8%), 13660–13627 (5.0%), 13616–13482calBP (83.6%)
3	IAAA-181203	S51 (lower)	sediment	-21.25 ± 0.22	12,408 ± 38	14858–14264 (95.4%)
4	IAAA-181204	S51 (lower)	sediment	-23.46 ± 0.24	11,982 ± 36	14024–13905 (48.3%), 13895–13785 (47.2%)
5	IAAA-190124	S53	sediment	-22.01 ± 0.18	12,696 ± 43	15278–14990 (95.4%)
6	IAAA-190125	S50	sediment	-25.56 ± 0.23	7,292 ± 31	8174–8025 (95.4%)
7	IAAA-190126	S51 (lower)	sediment	-24.14 ± 0.19	12,001 ± 43	14025–13793 (95.4%)
8	TKA-20364	S10 (lower)	charcoal	-27.5 ± 0.5	3,867 ± 24	4409–4231 (88.6%), 4200–4180 (4.7%), 4170–4158 (2.2%)
9	TKA-20365	S10 (upper)	charcoal	-25.6 ± 0.4	1,037 ± 21	961–917 (95.4%)
10	TKA-20366	S31	charcoal	-23.7 ± 0.5	5,833 ± 26	6735–6559 (95.4%)
11	TKA-20367	S63	charcoal	-22.7 ± 0.4	19,693 ± 56	23848–23709(63.2%), 23575–23406 (32.2%)
12	TKA-20368	S30 (upper)	charcoal	-29.8 ± 0.5	4,773 ± 26	5585–5469 (95.4%)
13	TKA-20369	S20	charcoal	-21.8 ± 0.8	4,506 ± 27	5300–5210 (30.9%), 5200–5048 (64.6%)
14	TKA-20460	S20	charcoal	-27.5 ± 1.0	4,699 ± 63	5581–5500 (23.2%), 5492–5315 (72.2%)
15	TKA-20461	S31	charcoal	-29.8 ± 1.0	5,191 ± 68	6183–6140 (6.9%), 6121–5855 (76.9%), 5828–5751 (11.6%)
16	TKA-21483	S10 (lower)	charcoal	-29.6 ± 0.2	4,535 ± 19	5314–5265 (29.6%), 5188–5052 (65.9%)
17	TKA-21484	00	charcoal	-25.5 ± 0.2	787 ± 16	726–678 (95.4%)
18	TKA-21485	S30 (lower)	charcoal	-28.4 ± 0.3	6,253 ± 21	7257–7156 (88.2%), 7113–7072 (6.3%), 7040–7032 (1.0%)
19	TKA-21486	S10 (upper)	charcoal	-25.8 ± 0.3	2,200 ± 20	2310–2143(92.9%), 2137–2126 (2.5%)
20	TKA-21487	S11	charcoal	-26.5 ± 0.2	2,213 ± 17	2315–2290 (13.7%), 2273–2149 (81.8%)
21	TKA-21488	S10	charcoal	-25.5 ± 0.3	3,178 ± 18	3447–3369 (95.4%)
22	TKA-21489	F00	sediment	-24.2 ± 0.2	9,609 ± 25	11164–11061 (23.2%), 11040–10998 (9.9%), 10972–10780 (62.3%)
23	TKA-21490	S30 (upper)	sediment	-28.1 ± 0.3	7,302 ± 23	8174–8030 (95.4%)
24	TKA-21491	S31	charcoal	-30.2 ± 0.3	7,229 ± 22	8167–8089 (20.3%), 8046–7969 (75.2%)

Supplement material 1: OxCal code for calculating the event ages of KMR trench

```
Plot()
 {
  Sequence()
  {
   Boundary("base");
   R_Date( "S53(5)" , 12696, 43);
   R_Date( "S51lower(3)" , 12408, 38);
   Date("E7");
   R_Date( "S51lower(7)" , 12001, 43);
   R_Date( "S5upper(2)" , 11722, 40);
   Date("E56");
   R_Date( "S50(1)" , 8634, 33);
   Date("E4");
   //Smith et al. (2013)
   Date("K-Ah", U(BC(5353),BC(5215)));
   Phase( )
   {
    R_Date("S31(10)", 5833, 26);
    R_Date("S31(15)", 5191, 68);
   };
   Date("E3");
   Phase( )
   {
    R_Date("S20(13)", 4506, 27);
    R_Date("S20(14)", 4699, 63);
   };
   Phase( )
   {
    R_Date("S10(25)", 4132, 32);
    R_Date("S10lower(16)", 4535, 19);
   };
   Date("E2");
   Phase( )
   {
    R_Date("S10lower(8)", 3867, 24);
    R_Date("S10(21)", 3178, 18);
    R_Date("S10upper(19)", 2200, 20);
   };
   Date("E1");
   R_Date("S10upper(9)", 1037, 21);
   R_Date("00(17)", 787, 16);
   Date("E0", AD(2016));
   Boundary("surface");
  };
```

```
90      RIE0_E7=(E0-E7)/7;
      };
```

Supplement material 2: OxCal code for calculating the event ages in Fig. 8.

```
Plot()
 {
//Miyaji Trench (Ishimura et al., 2021)
  Sequence(MYJ-Tr)
  {
   Boundary("base1");
   Sequence("bottom of 60")
   {
    R_Date( "bottom of 60" , 2640, 20)
    {
     z=118;
    };
    R_Date("top of 60", 2620, 20)
    {
     z=104;
    };
    R_Date("bottom of 400", 2070, 20)
    {
     z=86;
    };
   };
   Date("E1");
   Sequence()
   {
    R_Date("top of 40", 1900, 20)
    {
     z=57;
    };
    R_Date("10", 1180, 20)
    {
     z=24;
    };
   };
   Boundary("0 m grid");
  };

//Komori Trench (This study)
  Sequence(KMR-Tr)
  {
   Boundary("base2");
   Date("K-Ah1", U(BC(5353),BC(5215)));
   Phase( )
   {
    R_Date("S31(10)", 5833, 26);
```

```
          R_Date("S31(15)", 5191, 68);
        };
        Date("E3");
        Phase( )
        {
          R_Date("S20(13)", 4506, 27);
          R_Date("S20(14)", 4699, 63);
        };
        Phase( )
        {
          R_Date("S10(25)", 4132, 32);
          R_Date("S10lower(16)", 4535, 19);
        };
        Date("E2");
        Phase( )
        {
          R_Date("S10lower(8)", 3867, 24);
          R_Date("S10(21)", 3178, 18);
          R_Date("S10upper(19)", 2200, 20);
        };
        Date("=E1");
        R_Date("S10upper(9)", 1037, 21);
        R_Date("00(17)", 787, 16);
        Date("E0", AD(2016));
        Boundary("surface");
      };

    //Futa Trench (Ishimura et al., 2022)
      Sequence( "Futa trench")
      {
        Boundary("base3");
    //Smith et al. (2013)
        Date("K-Ah2", U(BC(5353),BC(5215)));
        Phase("unit41_Tr2-2")
        {
          R_Date("TKA-23226", 5288, 24);
          R_Date("TKA-23228", 5326, 24);
        };
        Date("=E3");
        R_Date("TKA-23236", 3901, 38);
        Date("=E2");
        R_Date("TKA-23222", 2825, 21);
        Phase("unit32")
        {
          R_Date("IAAA-191939", 2780, 26);
          R_Date("IAAA-192204", 2216, 23);
```

```
        R_Date("IAAA-192205", 2456, 23);
        R_Date("TKA-22034", 2225, 21);
        R_Date("TKA-22037", 2178, 20);
        R_Date("TKA-23221", 2215, 20);
        R_Date("TKA-23229", 2172, 21);
      };
      Date("=E1");
      Phase("unit31")
      {
       R_Date("TKA-22038", 1340, 19);
       R_Date("TKA-22041", 1579, 20);
      };
      Phase("unit30")
      {
       R_Date("IAAA-192202", 917, 22);
       R_Date("IAAA-192209", 969, 21);
       R_Date("TKA-22040", 954, 20);
       R_Date("TKA-22042", 954, 21);
      };
      Phase("unit12")
      {
       R_Date("TKA-22043", 103, 18);
      };
      Boundary( "=E0");
    };
    Page();
    // Calculate intervals between seismic events & summed interval distribution (ID)
    Sum("ID")
    {
     I0_1=E0-E1;
     I1_2=E1-E2;
     I2_3=E2-E3;
    };
  };
```